Visualization of Knocking Combustion in a Hydrogen Spark-Ignition Engine

M. Kanti Roy, N. Kawahara, E. Tomita

This document appeared in

Detlef Stolten, Thomas Grube (Eds.):
18th World Hydrogen Energy Conference 2010 - WHEC 2010
Parallel Sessions Book 6: Stationary Applications / Transportation Applications
Proceedings of the WHEC, May 16.-21. 2010, Essen
Schriften des Forschungszentrums Jülich / Energy & Environment, Vol. 78-6
Institute of Energy Research - Fuel Cells (IEF-3)
Forschungszentrum Jülich GmbH, Zentralbibliothek, Verlag, 2010
ISBN: 978-3-89336-656-9

Visualization of Knocking Combustion in a Hydrogen Spark-Ignition Engine

Mithun Kanti Roy, **Nobuyuki Kawahara**, **Eiji Tomita**, Okayama University, Japan

1 Introduction

Internal combustion engines which use hydrogen as a fuel will play a major role in the future automotive propulsion systems. Hydrogen has a wide flammability range and high burning velocity for combustion in a Spark-ignition (SI) engine. Its wide flammability range provides smooth engine operation at a very lean mixture with a low NO_x level. In addition, its high burning velocity may contribute to a relatively high thermal efficiency with a shorter combustion period at the ignition timing close to top dead centre (TDC). However, the extremely rapid combustion of hydrogen causes abnormal burning such as knocking, pre-ignition and backfiring at higher loads reducing the engine reliability and limiting the engine power [1]. Numerous investigations have shown that the onset of knock, which is caused mainly by the autoignition of the unburned end-gas before being consumed by the propagating flame. The autoignition of the end-gas also creates a rapid increase in pressure, which sets up a pressure wave that impulsively acts against the cylinder walls and then oscillates at the resonant frequency about 5-7 kHz [2]. The aim of this work is the investigation of the phenomena occurring during the knock initiation and development period through the visualization and spectrum analysis in a hydrogen spark-ignition engine. A specially designed hydrogen fuels rapid compression and expansion machine (RCEM) that could only be fired once was used for the experiment. The experiments clearly show that the location where autoignition occurred was identified from the high speed direct images by their brightness in the end-gas region. The chemical luminescence emissions such as OH* radical were detected due to hydrogen oxidation during knocking combustion.

2 Experimental Apparatus and Method

In this study, RCEM that can only be fired once was used to investigate end-gas autoignition and combustion characteristics of hydrogen. The bore and stroke of RCEM are 78 mm and 85 mm respectively with a pancake combustion chamber and a compression ratio of 9.0:1. The engine was operated at 600 rpm by a controllable electric motor. Figure 1 shows a schematic diagram of the experimental set-up used in this study. Initially, a homogeneous H_2-O_2-Ar mixture was introduced into the mixture tank and engine cylinder, which were connected by a pipe, at an initial pressure P_0 through an open valve with the piston set at TDC. The specific heat ratio of Ar gas is much higher than that of N_2 so that in-cylinder mixture temperature at the TDC is much higher than that of air. The initial pressure P_0, of the mixture was varied from 40 to 60 kPa and the initial temperature was maintained at 323 K. The pre-mixed gas was ignited by an electric spark at crank angle θ_{IT}. In-cylinder pressure was measured with a Kistler 6052C piezo-electric transducer. The RCEM has a cylindrical quartz window 32 mm in diameter positioned on the top of the cylinder head. The window is on the opposite side from the spark electrode as shown in Fig. 1. In-cylinder combustion

images were captured by two types of high-speed video cameras: a high-speed colour video camera (Memrecam GX-1, NAC Image Technology) with a resolution dependent on the camera speed, and a monochrome camera (HPV-1, Shimadzu Hyper Vision) with a resolution of 316 × 260 pixels. Chemiluminescence signal was obtained using two spectrometers (Oriel MS257™ and Andor Technology SR 163i) equipped with an Intensified CCD (Andor Technology, DK720-18F-04, 1024 X 156 pixels).

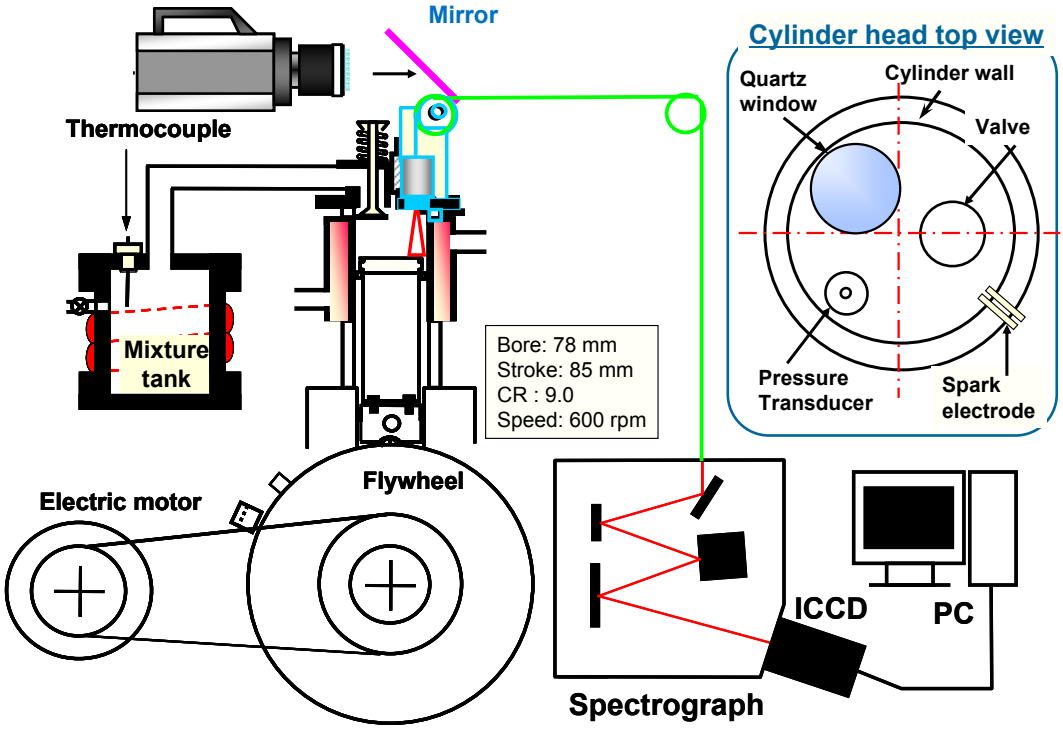

Figure 1: Schematic diagram of the specially designed rapid compression-expansion machine with a high-speed photography and spectroscopy system.

3 Result and Discussion

Combustion in an SI engine can occur as a normal or abnormal phenomenon, depending on the engine operating condition. In this experiment, H_2-O_2-Ar mixtures developed different pressure histories during knock combustion due to differences in the energy release rate, which was affected by the amount of unburned fuel and the mixture composition in the end-gas. Figure 2(a) shows a pressure versus crank-angle diagram plotted using in-cylinder pressure data. Here knock is distinguished by strong pressure oscillations that occur near the maximum pressure and continue for part of the expansion stroke. Pressure pulsation in engine cylinders - during normal combustion in a SI engine cylinder pressure progressively increase during combustion process. In knocking combustion, a sharp increase in pressure occurs when the end-gas is autoignited before the flame front reaches the cylinder wall. The knock intensity (KI) in this research work was calculated using the pressure data by using digital butterworth band-pass filter with 2.5 kHz cutoff frequency. KI has to be defined, peak of the oscillation component of in-cylinder pressure. Figure 2(b) shows the filtered pressure

traces with marking describing the point used for calculating KI. The rate of pressure rise had a discontinuity at the knock occurring crank angle and the bandpass-filtered signal started to increase just after the onset of knock.

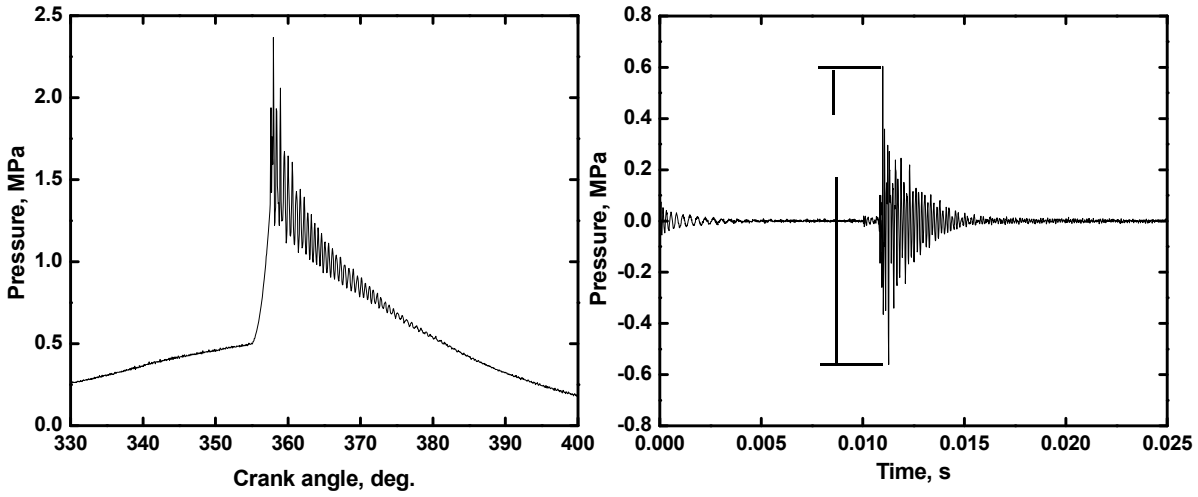

(a) In-cylinder pressure oscillation. **(b) Time-series of knock intensity, KI**

Figure 2: In-cylinder pressure history and the knock intensity. (H_2-O_2-Ar, Φ =1.0, θ_{IT}=355°, P_o=40kPa)

In general, pressure measurements provide global information and do not indicate the species involved in knocking. Figure 3 shows the time-series images at a specific crank angle for both normal and knocking combustion cycles with typical in-cylinder pressure histories. The upper images of this figure correspond to the normal combustion cycle (H_2+air mixture) whilst the lower images correspond to the knocking combustion cycle (H_2+O_2+Ar mixture). During the normal cycle after the spark ignition, a premixed low luminous flame was observed. Figure 3 shows that the flame gradually propagated from the lower right side to the upper left side of the combustion image (frames A to D). Flame front propagation for the normal cycle was very smooth and no signs of autoignition were visible in the end-gas region.

In the knock cycle after the spark ignition, a spark-initiated blue-colour flame propagates into the end gas, in which preknock oxidation develops. During this process it is noticed that flame hesitates to propagate into the end-gas and a propagating flame does not spread as a semicircular flame front in a uniform way across the combustion chamber. A wedge-shape end-gas is always produced ahead of the flame front retardation in knocking cycle. It is assumed that the “stressed” end-gas will give a chemical inhibitory effect and cause the slowing down of the incoming propagating flame, this provide sufficient time for the end-gas autoignition. The autoignited kernel of the end-gas appeared in front of the propagating flame in the upper left corner of the frame G in Fig. 3. At the instance of knock, corresponding to frame H, the unburned end-gas region suddenly flashed white and expanded towards the

burned gas region with high density pressure waves. The propagation of abnormal combustion is caused by autoignitive pressure wave [3].

The effect of cycle-to-cycle variation of engine combustion was evaluated by comparing knocking images for the same ignition timings, as shown in Fig. 4. The autoignition location near the cylinder wall fluctuated cycle-to-cycle, but remained inside the end-gas region, which was compressed by the propagating flame front. The exact location where autoignition occurred was identified from the high-speed color images by their brightness. In this experiment cylinder wall temperature was very low but most of the time the knock was generated in the end-gas region near the cylinder wall. We found that in hydrogen SI engine combustion at condition applied in this experiment, the knock occurrence region is near the cylinder wall in the end-gas region.

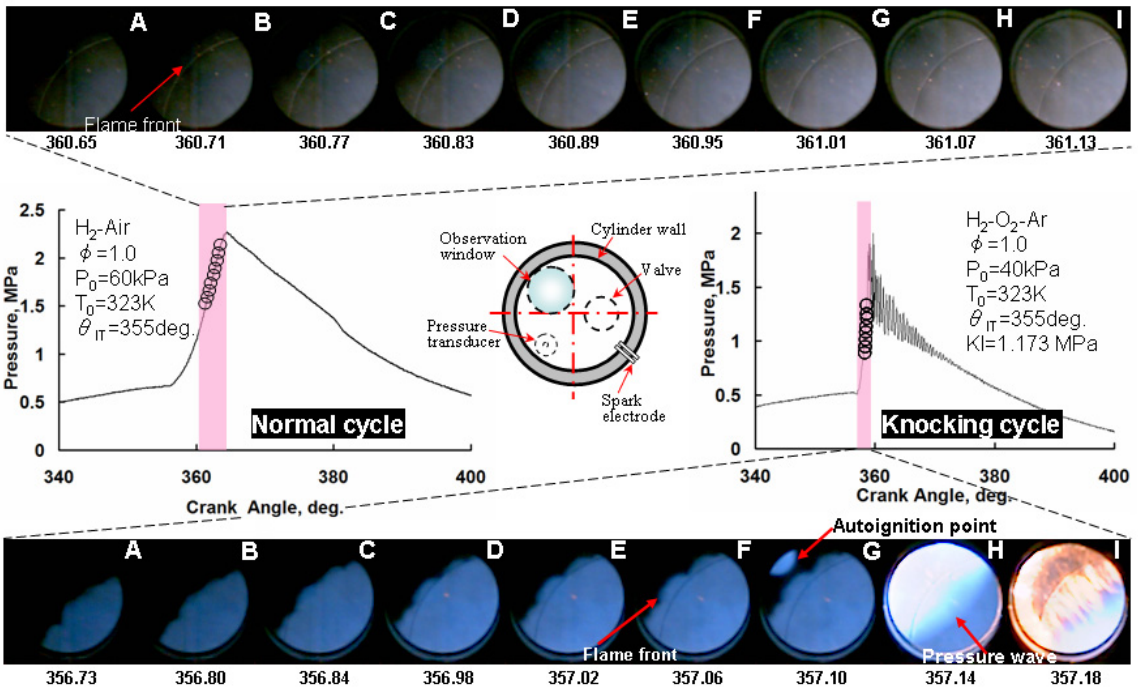

Figure 3: Time-series direct combustion images, including in-cylinder pressure histories for normal and knocking cycle taken at 80,000 frames per second.

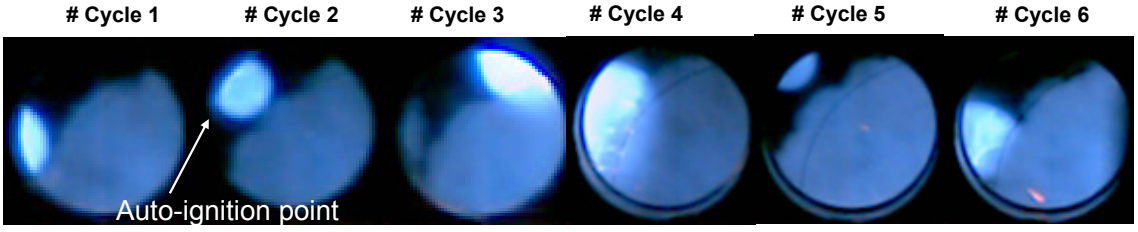

Figure 4: Cycle-to-cycle combustion images with the autoignited kernel in the end-gas region. (H_2-O_2-Ar, Φ =1.0, θ_{IT}=355°, P_o=40kPa)

Figure 5 shows the KI for different combustion cycles has a close relationship with the mass fraction of the unburned end-gas mixture and the autoignition temperature evaluated from the in-cylinder pressure. The volume of the unburned region could be estimated from the high-speed color images. The volume of the unburned region was determined from the image obtained before the appearance of autoignition inside the end-gas region. The volume of the unburned region was defined as (S0–S)x H, where S is the burned region obtained from the visualized images, S0 is the total area of the image, and H is the height of the combustion chamber. The mass of the unburned mixture was obtained using the mixture density estimated from the unburned gas temperature and volume. Figure 5(a) shows that large amount of the unburned end-gas mass leads the higher KI. Spark-initiated flame propagates into the end-gas in which preknock oxidation develops. The unburned gas temperature was estimated using the in-cylinder pressure with a two-zone model [4]. Autoignition occurred at the point with the maximum temperature, and then propagated throughout the entire volume. Figure 5(b) shows the relationship between the autoignition temperature and KI. Higher end-gas temperatures increased the autoignition reaction process and increased the chance of knocks occurring. Based on the captured images, it can be confirmed that the KI was strongly related to the mass fraction of the unburned end-gas and autoignition temperature.

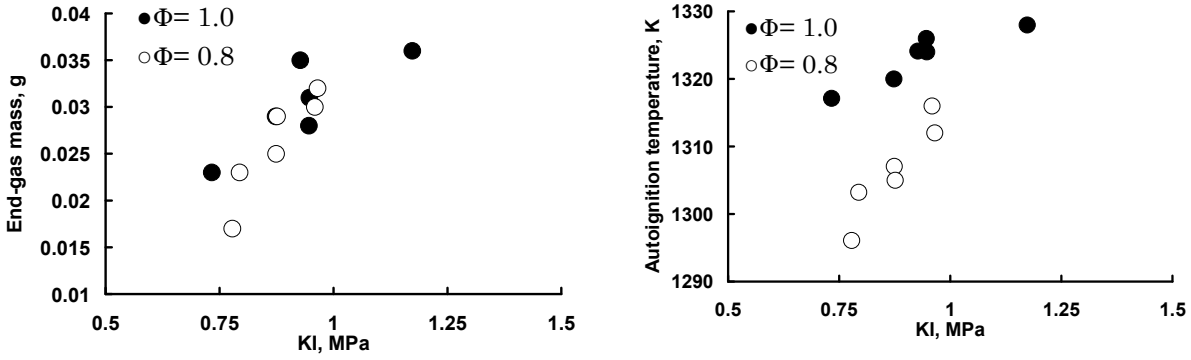

(a) End-gas mass **(b) Autoignition temperature**

Figure 5: KI relationship between the unburned end-gas mass and the autoignition temperature. (H_2-O_2-Ar, θ_{IT}=355°, P_o=40kPa)

The chemiluminescence emissions of the normal propagating flame and burned gas before and after the autoignition of the end-gas were obtained using spectrometer equipped with an ICCD. The measurement location was set based on the higher frequency occurrence of auto-ignition inside the end-gas region. Chemiluminescence is the natural light emission as the energy released from chemical reaction. The reaction mechanism for hydrogen combustion is rather easy compared with hydrocarbon combustion, leaving only OH* radical emission as the only practical measurement path. These excited species emit photon at discrete wavelength as they moved from higher excited energy states to lower energy state. Figure 6 shows the overall spectrum for knocking cycle obtained between wavelength of 200 and 800 at the end-gas and burned gas measurement location. This figure shows that OH radical

emission was detected in the UV spectra near 309.4 nm as the energy released during chemical reaction before the end-gas autoignited and in the burned gas region there are two other peaks such as sodium (Na) and potassium (K) near 589 and 767 nm respectively.

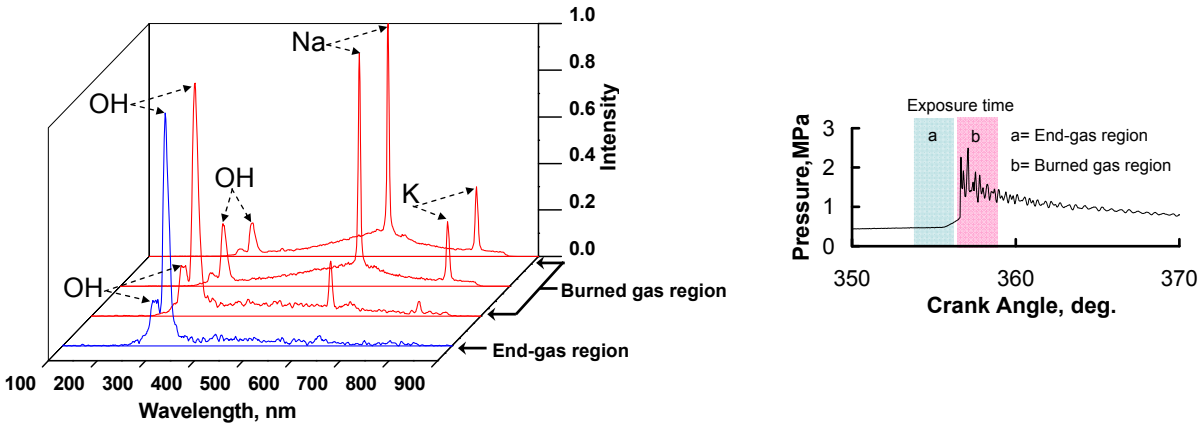

Figure 6: Overall spectral profile for the end-gas and burned gas region during knocking cycle. (H_2-O_2-Ar, Φ =1.0, θ_{IT}=355°, P_o=40kPa; Grating= 150 line/mm, Center wavelength= 500nm, Exposure time= 2ms)

The emission peaks of Na and K may be attributing to the combustion of lubricating oil that was noticed from the high-speed combustion images. The water molecule (H_2O) is very stable and may assume to be formed at about over 600 nm as the end product of the reaction possessing excessive energy. Figure 7 shows the overall spectrum for non-knocking cycle combustion obtained between wavelength of 200 and 800 nm at the burned gas region. As shown, there are two significant peaks of OH radical in UV spectra and also other emission peaks of Na (near 589 nm) and water vapor (over 600 nm). At the end stage of the burned gas region during non-knocking combustion, the other peak of K at 770 nm was detected as shown in Fig. 7. Figure 8 shows the UV spectra band of OH* radical emissions at knocking combustion during different periods, before and after autoignition. There are four strong main band heads R1, R2, Q1 and Q2 at 306.36 nm, 307.77 nm, 307.88 nm and 309.04 nm respectively, corresponding to the diatomic molecular transition ($A\,^2\sum \rightarrow X\,^2\prod$) [5]. As shown in Fig. 8 two bands of OH* radical emission were detected just before the autoignition at wavelengths of 282 and 307.84 nm, is the indication of the knock onset. It is thought that the flame doesn't reach the measurement point because there is a possibility of flame reflection. When the end-gas pressure and temperature increased sufficiently high by the compression of propagating flame front, then the OH* radical may be produced by thermal excited radical. Figure 8 also shows that after the autoignition OH* radical emission intensity becomes stronger with increasing pressure and temperature in the knocking combustion.

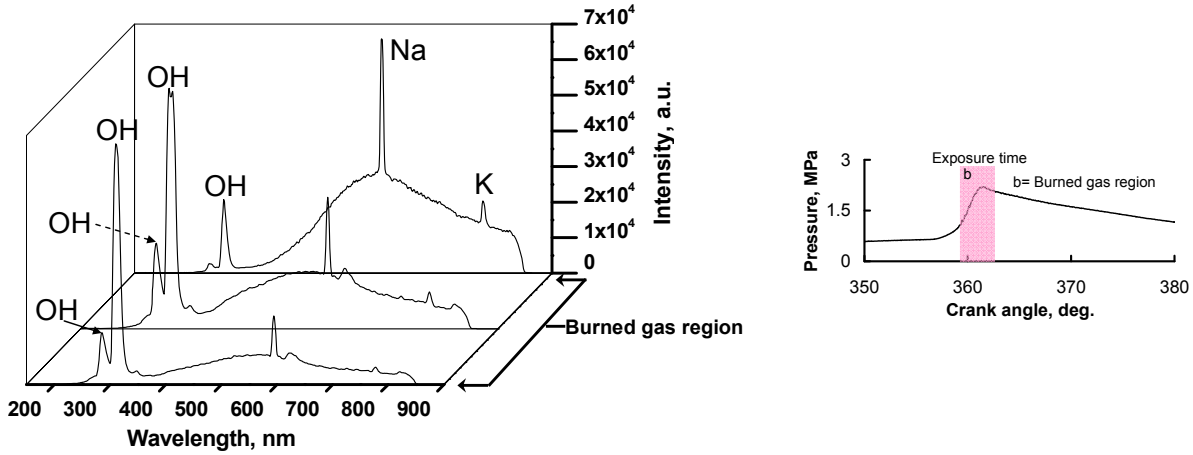

Figure 7: **Overall spectral profile for the burned gas region during non-knocking cycle. (H_2-Air, Φ =1.0, θ_{IT}=355°, P_o= 60kPa; Grating= 150 line/mm, Center wavelength= 500nm, Exposure time= 2ms)**

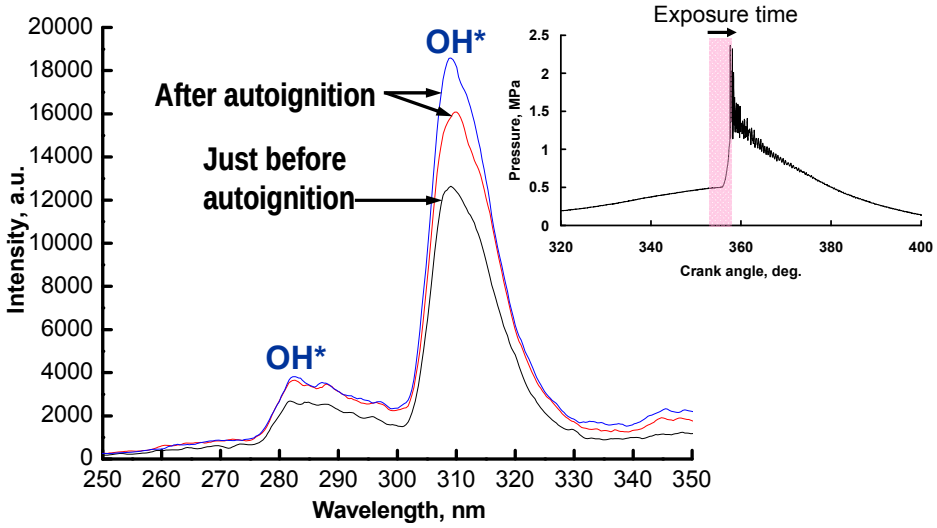

Figure 8: **Experimental typical OH* spectra at just before and after knock combustion. (H_2-O_2-Ar, Φ =1.0, θ_{IT}=355°, P_o=40kPa; Grating= 300 line/mm, Center wavelength= 350nm, Exposure time= 2ms)**

4 Conclusions

In this study, the experiments with RCEM were conducted to investigate autoignition and combustion behavior of hydrogen fuel based on in-cylinder pressure measurements, high-speed imaging and spectroscopy analysis. The following conclusions should be drawn from this experiment:

1. During knocking combustion, the autoignited kernel of the end-gas region that was compressed by the propagating flame front could be visualized. The direct photography can detect the precise position and brightness of the combustion flames that can not be observed by shadowgraph.
2. A large amount of unburned end-gas and a higher autoignition temperature has a good relationship with an increased KI.
3. We try to understand the hydrogen oxidation before the end-gas autoignition with the help of emission spectroscopy analysis. In the end-gas region OH* radical is the indication of the onset of hydrogen oxidation.

References

[1] A. Mohammadi, M. Shojo, Y. Nakai, W. Ishikura, E. Tabo, Performance and Combustion Characteristic of a Direct Injection SI Hydrogen Engine. International Journal of Hydrogen Energy, Volume 32(2007), Issue 2, pp. 296-304.

[2] N. Kawahara, E. Tomita, Visualization of auto-ignition and pressure wave during knocking in hydrogen spark-ignition engine. International Journal of Hydrogen Energy, Volume 34(2009), pp. 3156-3163.

[3] D. Bradley, G.T. Kalghatgi, Influence of autoignition delay time characteristics of different fuels on pressure waves and knock in reciprocating engines. Combustion and flame 156(2009), pp.2307-2318.

[4] J.B. Heywood, Internal Combustion Engine Fundamentals: McGraw-Hill Book, Inc., 1988

[5] A.G. Gaydon, The spectroscopy of flames, 2nd edition 1974 (Chapman & Hall, London), pp.364-365.